

# Phase Evolution in the $\text{Fe}_3\text{O}_4\text{-Fe}_2\text{TiO}_4$ Pseudo-Binary System and Its Implications for Remanent Magnetization in Martian Minerals

Adam Wise<sup>1</sup>, Maryanna Saenko<sup>1</sup>, Amanda M. Velázquez<sup>1</sup>, David E. Laughlin<sup>1,2</sup>, Marina Díaz-Michelena<sup>3</sup>, and Michael E. McHenry<sup>1</sup>

<sup>1</sup>Materials Science and Engineering Department, Carnegie Mellon University, Pittsburgh, PA 15213 USA

<sup>2</sup>ALCOA Professor of Physical Metallurgy, Carnegie Mellon University, Pittsburgh, PA 15213 USA

<sup>3</sup>Space Programs and Space Sciences Department, Instituto Nacional de Técnica Aeroespacial (INTA), Madrid, 28850 Spain

**Titanomagnetites offer a rich system to explore the role of fine microstructure on magnetic properties. They are important minerals in basalts, and are commonly found on the moon and Mars. Here magnetic measurements were used to monitor decomposition and phase evolution in the pseudo-binary  $\text{Fe}_2\text{TiO}_4\text{-Fe}_3\text{O}_4$  solid solution system. The phases appearing in the decomposition are a strongly magnetic magnetite and a weakly magnetic Ti-rich spinel. For the 40, 50, and 60 at%  $\text{Fe}_2\text{TiO}_4$  compounds (balance  $\text{Fe}_3\text{O}_4$ ) explored here, a metastable solid solution is nonmagnetic at temperatures where decomposition kinetics can be monitored in reasonable experimental times. The magnetization of magnetite formed by the decomposition offers a direct measure of the volume fraction transformed. Time-dependent magnetization measurements were used to monitor the kinetics of decomposition and compared to models for spinodal decomposition and nucleation and growth kinetics for compositions outside the spinodes. The fine microstructure resulting from spinodal decomposition and exchange bias mechanisms for coupling, may be important in understanding the remnant state of these minerals on Mars.**

**Index Terms**—Magnetic materials, magnetometry, Mars, phase separation, spinels.

## I. INTRODUCTION

**T**ITANOMAGNETITES are a rich system to explore the role of fine microstructure on magnetic properties. They are important minerals in basalts and commonly occur on the earth [1], the moon [2] and Mars [3]. The remanent state of these minerals is hypothesized to contribute to planetary field anomalies and provides clues for the geomagnetic evolution of planets [4]. The important contribution of these minerals to local remanent magnetizations argues for their importance in magnetic surveying efforts [5]. The minerals give information to the existence of water coupled to the origin of life on planets. For example, magnetic particles detected in the Martian atmosphere are hypothesized as originating from titanomagnetite occurring in palagonite inherited from a basaltic precursor [6].

This work uses magnetic measurements to probe the phase evolution in the decomposition of solutions in the pseudo-binary  $\text{Fe}_2\text{TiO}_4\text{-Fe}_3\text{O}_4$  system with the goal of providing information useful for understanding the origin of terrestrial and extraterrestrial magnetic field anomalies. This pseudo-binary system has a miscibility gap with spinodal decomposition [7], [8]. Solid solutions decompose into magnetite and a more weakly magnetic Ti-rich spinel. At many compositions, a homogeneous metastable solid solution is nonmagnetic at temperatures where decomposition kinetics can be monitored in reasonable times. Temperature dependent magnetization measurements identify the phases evolving. The magnetization of magnetite formed by decomposition is a measure of volume fraction transformed. Time-dependent magnetization measurements monitor kinetics of spinodal decomposition for compositions in the spinodes and

nucleation and growth kinetics for compositions outside of the spinodes to more accurately define the asymmetric miscibility gap.

A fine microstructure resulting from spinodal decomposition and exchange related coupling may explain a large remanent state for these minerals on Mars. Certain compounds are of further interest as they have magnetic transitions in the day to night temperature swing on Mars (and the moon) and can be detected with miniaturized magnetic sensors [9] and identified on the basis of their transition temperatures. The mineral magnetization is important to current Mars exploration efforts [10].

## II. EXPERIMENTAL PROCEDURE

We have developed synthesis routes for compounds in the pseudo-binary  $\text{Fe}_2\text{TiO}_4\text{-Fe}_3\text{O}_4$  system that allow us to more accurately define its asymmetric miscibility gap. The mixtures used to synthesize the  $\text{Fe}_3\text{O}_4\text{-Fe}_2\text{TiO}_4$  pseudobinary alloys used in this study were made by mixing the two endpoint materials.  $\text{Fe}_3\text{O}_4$  was purchased commercially, with 99.9% purity.  $\text{Fe}_2\text{TiO}_4$  was synthesized by combining stoichiometric amounts of  $\text{TiO}_2$ ,  $\text{Fe}_2\text{O}_3$ , and Fe sponge. According to Wechsler [11] *et al.*,  $\text{Fe}_2\text{TiO}_4$  synthesized in this way tended to be Fe-deficient, so 3 at% extra Fe sponge was added to this mixture. The mixture was ball-milled for 15 minutes per batch using steel spheres in a 10:1 mass ratio with the powder to reduce the particle sizes and thoroughly homogenize the powders. Once ball milling was complete, the mixture was pressed into pellets. The pressed pellets were loaded into Fe crucibles and heated in a tube furnace for 60 h at 1050°C under an Ar atmosphere to prevent oxidation. The composition of the pellets was verified via XRD as being  $\text{Fe}_2\text{TiO}_4$  with small amounts of residual ilmenite.

$\text{Fe}_2\text{TiO}_4$  pellets were reball-milled for 2 min. per batch with a 10:1 mass ratio of steel spheres to pellets to break up the pellets and produce powder suitable for mixing with the commercial

Manuscript received February 18, 2011; accepted May 13, 2011. Date of current version September 23, 2011. Corresponding author: A. Wise (e-mail: adam-wise@andrew.cmu.edu).

Color versions of one or more of the figures in this paper are available online at <http://ieeexplore.ieee.org>.

Digital Object Identifier 10.1109/TMAG.2011.2157471

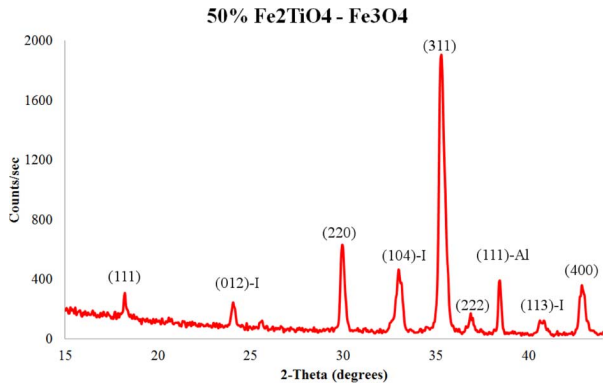


Fig. 1. XRD powder pattern taken from the 50%  $\text{Fe}_2\text{TiO}_4\text{-Fe}_3\text{O}_4$  solid solution sample after synthesis but before annealing. The peaks with the ‘-I’ postscript are ilmenite peaks, and the peak with the ‘-Al’ postscript is an aluminum peak caused by the sample holder.

$\text{Fe}_3\text{O}_4$  powder. Powers with 40, 50, and 60 at%  $\text{Fe}_2\text{TiO}_4$  and the balance  $\text{Fe}_3\text{O}_4$  were mixed to prepare single-phase pseudobinaries. The precursors were ball-milled for 15 minutes using a 10:1 mass ratio of steel balls to powder and placed in Fe crucibles before being placed in a tube furnace at  $950^\circ\text{C}$  for 60 h under an Ar atmosphere. Powders furnace cooled under an Ar atmosphere until  $400^\circ\text{C}$ , then removed to air-cool to room temperature. Powders were verified to be single-phase using a Panalytical X’Pert XRD equipped with a PIXCel detector and a Cu radiation source. Fig. 1 shows results for the 50%  $\text{Fe}_2\text{TiO}_4\text{-Fe}_3\text{O}_4$  alloy, as well as the peaks for residual ilmenite. The aluminum peak labeled is due to the sample holder.

$\text{Fe}_3\text{O}_4\text{-Fe}_2\text{TiO}_4$  solid solutions were powdered for magnetic examination. Measurements were performed on a Lake Shore 7404 VSM system. M vs. H loops were taken with a range of 5000 Oe and M vs. T scans were also recorded under a 5000 Oe field from room temperature to  $600^\circ\text{C}$  using a furnace attachment with the sample chamber under flowing Ar.

Powder microstructures were determined by TEM. Samples were first heat-treated at  $400^\circ\text{C}$  for 24 h while encapsulated in silica glass. The samples were then shattered. Sharp shards resulting from the shattering were mounted to copper sample holders and placed in an FEI Novalab 600 Focused Ion Beam (FIB) system for thinning. The sharp edge of the shard was mounted facing out so that the FIB was able to thin the sharp edge to electron transparency. FIB thinned samples were characterized on an FEI Tecnai F20 microscope equipped with an Orius SC600 CCD for image capture. The microscope was operated in STEM mode for analytical work, and had an EDAX Energy Dispersive X-ray (EDX) system for compositional analysis. High angle annular dark field (HAADF), also referred to as Z-contrast images, were used to image grain structure. EDX line scans and maps were taken to extract composition data.

### III. RESULTS AND DISCUSSION

Saturation magnetizations in the pseudo-binary  $\text{Fe}_2\text{TiO}_4\text{-Fe}_3\text{O}_4$  system depend on the composition and cation site occupancies. Titanomagnetites can deviate from ideal stoichiometries due to: 1) exsolution as discussed here; 2) nonstoichiometry at high and low temperatures, and 3) cation impurities [12]. The last of these are not considered here as

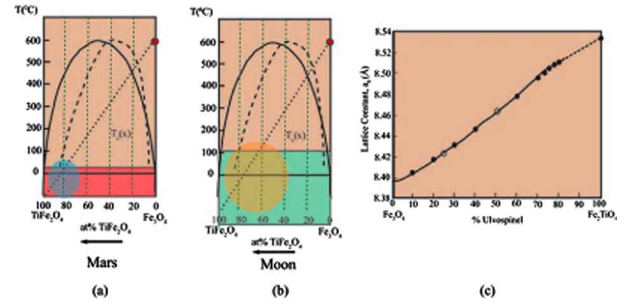


Fig. 2. Calculated phase diagram of magnetite-ulvospinel alloy. The solid lines show predicted miscibility gaps from regular solution theory and the dashed curve is an experimentally determined miscibility gap. The dotted line is the magnetic (TN) transition. The red area in (a) represents the day-to-night temperature swing on Mars and the green area in (b) on the lunar surface. (c) Lattice constant variation with composition for magnetite-ulvospinel solid solutions.

the materials were synthesized from relatively pure species. A general cation distribution in homogeneous and stoichiometric titanomagnetites is given by the formula

$$\left( \text{Fe}_{(2-2x)\alpha}^{3+} \text{Fe}_{1-(2-2x)\alpha}^{2+} \right) \cdot \left[ \text{Fe}_{(2-2x)(1-\alpha)}^{3+} \text{Fe}_{x+(2-2x)\alpha}^{2+} \text{Ti}_{1-x}^{4+} \right] \text{O}_4^{2-} \quad (1)$$

where  $x$  denotes the molecular fraction of ulvospinel,  $( )$  denotes A-site cations and  $[ ]$  B-site cations and  $\alpha$  is the degree of inversion [12]. Magnetization data has been interpreted in terms of a thermally activated degree of inversion,  $\alpha(T)$  [12]. However, the activation energy barrier for this inversion is remarkably similar to the activation energy for Fe tracer diffusion ( $\sim 0.5$  eV/atom) [13], [14]. Magnetite cation diffusion energy barriers are largely determined by the formation energies for Frenkel defects on the Fe cation sublattices ( $\text{Fe}_{\text{Fe}} \rightarrow \text{V}_{\text{Fe}}'' + \text{Fe}_{\text{Fe}}'$ ) as expressed in the standard Kroger-Vink notation [15]. The thermally activated growth in the magnetization of titanomagnetite solid solutions has been used to monitor the diffusion kinetics [13]. These diffusive mechanisms for and consequent changes in magnetization strongly suggest that the inversion rate kinetics actually are probing exsolution kinetics. It is important to distinguish between exsolution by nucleation and growth kinetics and that occurring by spinodal decomposition. The former requires overcoming an additional barrier to nucleation and long range diffusion. The latter begins spontaneously and requires only short-range diffusion to proceed.

Fig. 2 shows a calculated phase diagram for the pseudobinary titanomagnetite system, generated by following Price’s method [16]. This calculation assumes a regular solution. The diagram is overlaid with a Vegard’s Rule estimation of the Néel temperature of the pseudo-binary system, ranging from  $575^\circ\text{C}$  for  $\text{Fe}_3\text{O}_4$  to 0 K for antiferromagnetic  $\text{Fe}_2\text{TiO}_4$ . Asymmetry in the miscibility gap in the titanomagnetites is an open question. The T-dependence of the magnetic transition for the solid solution series between magnetite and ulvospinel shows the magnetite phase is magnetic at all temperatures in the day-to-night temperature swing on Mars (a) and the moon (b) for a symmetric as well as an asymmetric miscibility gap. On the other hand the Ti-rich phases developed in exsolution may go through magnetic transformations in these day-to-night temperature swings

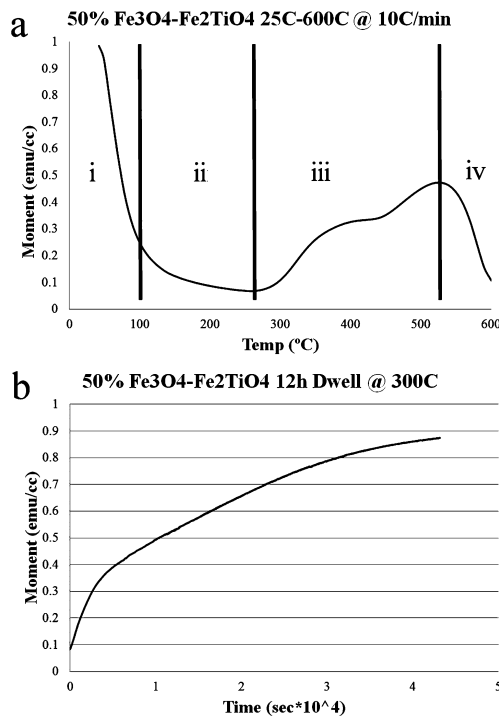


Fig. 3. Magnetic behavior of 50% ulvospinel (balance magnetite). (a) Four regimes are distinguished and used to track phase evolution: i) solution below its Néel temperature, ii) solution above its  $T_N$ , iii) phase separation with magnetite below its  $T_N$ , and iv) two phases above magnetite's  $T_N$ . (b) Isotherm at 300°C and 5000 Oe for the same composition. The suggested absence of an incubation period may signal spinodal decomposition is operative.

depending on their state of decomposition. Both magnetite and ulvospinel are cubic inverse spinels and the lattice constant of solid solutions varies linearly with composition in the pseudobinary system.

Reference to Fig. 2 is useful in explaining the behavior of the system seen in Fig. 3(a). In Fig. 3(a), the  $M$  vs.  $T$  curve (during heating) for the 50% Fe<sub>2</sub>TiO<sub>4</sub> sample is shown. The sample starts as a single phase solution as confirmed by XRD results. The phase evolution of the samples on heating is broken into four regions, as illustrated in Fig. 3(a). In the first region, marked 'i' on the diagram, the sample is below the Néel temperature ( $\sim 100^\circ\text{C}$ ) of the solid solution estimated from the Vegard's Rule interpretation of Fig. 2. The moment drops monotonically as the sample is heated to 100°C. Above this temperature, the region marked 'ii' on the diagram, a very small residual magnetization is seen, possibly associated with a small amount of unreacted Fe in the sample undetectable by XRD.

In region iii of the  $M$  vs.  $T$  curve, the sample moment increases as phase separation in the sample begins. With increasing temperature the kinetics of phase separation are enhanced, resulting in a two-phase mixture, ultimately with compositions at either edge of the miscibility gap. The material forming with a composition close to Fe<sub>3</sub>O<sub>4</sub> is below its Néel temperature; thus, the magnetic moment increases as the volume fraction of the magnetic magnetite phase increases. Finally, in region iv of the  $M$  vs.  $T$  curve, the sample passes through the Néel temperature of pure Fe<sub>3</sub>O<sub>4</sub> ( $\sim 575^\circ\text{C}$ ), and the magnetic response falls again. This  $M(T)$  response suggests the

kinetics of phase separation can be monitored by monitoring the magnetic response of the sample on heating.

Fig. 3(b) shows the isothermal magnetization of the 50% Fe<sub>2</sub>TiO<sub>4</sub> sample as a function of time at 300°C in an Ar atmosphere with an applied field of 5000 Oe. This temperature was chosen, since Fig. 3(a) suggests it would have a fairly slow reaction rate, limited by kinetics. The  $M(t)$  measurement in Fig. 3(b) was begun by a fast ramp to 300°C, at 20°C/min. It follows the reaction as it proceeds; the signal from the sample increases exponentially with time.

When precipitation of a magnetic phase occurs in a nonmagnetic host at an isothermal transition temperature, the magnetization is proportional to the volume fraction transformed,  $X(t)$ , and serves as a measure of transformation kinetics [17]. For JMAK kinetics, the isothermal  $X(t)$  response has a characteristic sigmoidal shape as observed in the nanocrystallization of NANOPERM materials [17]. For spinodal decomposition, the absence of a nucleation barrier suggests that an early stage incubation step does not occur and the magnetization reflects the increase in Fe composition of the magnetic phase. The fact that this composition should be near the middle of the miscibility gap and that the kinetic curves do not exhibit a typical JMAK shape suggest that spinodal decomposition may be operative, and measurements reflect diffusion kinetics of the compositional evolution in the Fe-rich phase.

In Fig. 4(a), a HAADF image of the 50% Fe<sub>2</sub>TiO<sub>4</sub> sample annealed for 24 h at 400°C is shown. The HAADF mode in the microscope shows contrast variation from differences in thickness and atomic number. In these samples, the bright regions would indicate increased thickness or increased atomic percentage of iron. In Fig. 4(b), an EDX map of the concentration of Ti is shown. The brighter regions are richer in titanium. In the TEM image from Fig. 4(a), there are two clearly distinct types of grain present. The first type of grain is seen in the upper central portion of the figure and has a mottled appearance, indicating a substructure which would be expected in samples that have spinodally decomposed. The second type of grain is seen surrounding the central grain. These grains have a very smooth appearance in the HAADF image. The smooth surrounding grains indicates that the structure in the central grain is not an artifact of sample preparation, and that the contrast observed in the central grain represents real atomic mass contrast.

In the HAADF image, regions with increased iron concentration should appear lighter, and it can be seen that the grain boundaries have the highest amount of contrast. The grain boundary on the right of the image that appears highly inclined to the beam shows up very brightly, while the grain boundary on the left side of the image appears to have a much lower angle of inclination to the beam doesn't show nearly as much contrast. Hence, it appears that there is an excess of iron at the grain boundaries. This excess amount was not picked up in the EDX measurements. However, the EDX measurements only measure near the surface of the sample, while the HAADF signal has passed through the entire sample.

In Fig. 4(b), a map of the titanium concentration in the sample is shown. In the central grain, there is very little titanium, while it's present in the surrounding grains. From this it is suggested that this sample has undergone phase separation by nucleation

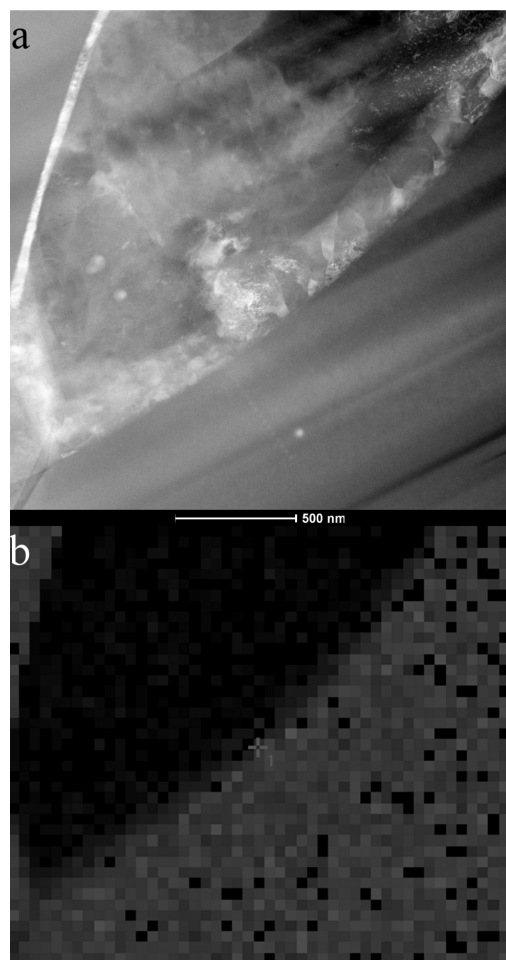


Fig. 4. (a) HAADF, or Z-contrast, image of a 50% ulvospinel (balance magnetite) sample. The lighter regions correspond to higher iron concentration and can be observed at the grain boundaries. (b) EDX map of same sample. In this case, the lighter regions represent higher titanium content.

and growth of new grains of different composition. The central grain has a composition very close to pure  $\text{Fe}_3\text{O}_4$ . While the approximately 22 at% Ti concentration in the surrounding grains indicates a composition of approximately 65%  $\text{Fe}_2\text{TiO}_4$  in the pseudobinary. This composition pair indicates that the assumption of a regular solution that has often been made in the literature is incorrect, as the miscibility gap appears to have a significant offset toward the  $\text{Fe}_3\text{O}_4$  side of the pseudo-binary.

Finally, it is noted that the sample used for TEM was heat-treated at higher temperatures and for much longer than that shown in the  $M(t)$  curve given in Fig. 3(b). This was done initially to guarantee that the phase separation reaction went to completion in the samples observed with TEM. The microstructure observed in the TEM clearly indicates phase separation via nucleation and growth. However, the lack of a nucleation plateau in Fig. 3(b), as well as the substructure apparent in the central grain in Fig. 4(a), indicate that this region undergone spinodal decomposition. With an asymmetric miscibility gap it is conceivable that the spinodal line passes through the 50 at% composition near 200-300 C and therefore some, especially heterogeneous, nucleation may occur.

#### IV. CONCLUSION

Pseudobinary alloys in the  $\text{Fe}_3\text{O}_4$ - $\text{Fe}_2\text{TiO}_4$  system have been analyzed and measured. These materials have been synthesized as single-phase materials, and have then been shown to phase-separate. This phase separation can be monitored via magnetic measurements. This magnetic monitoring offers a unique way of observing exsolution kinetics in this materials system. Phase separation by nucleation and growth has been confirmed via TEM. Analytical TEM work shows that the miscibility gap of the system is offset toward the  $\text{Fe}_3\text{O}_4$  side of the pseudobinary. Finally, indications are present that, while the system (given sufficient time) decomposes through nucleation and growth, the initial decomposition mechanism may be spinodal decomposition.

#### ACKNOWLEDGMENT

This work was supported in part by the NSF under Grants DMR0804020 and DMR1106943, as well as the Spanish National Space Program (DGI-MEC), Project MEIGA-MET-NET, Grant PJE-09001. The authors wish to acknowledge S. Patricopolous for help in sample synthesis and testing. As well as J. Wolf and T. Nuhfer of the J. Earl and Mary Roberts Center for Materials Characterization.

#### REFERENCES

- [1] C. Klein and C. S. Hurlbut, *Manual of Mineralogy*, 21st ed. Hoboken, NJ: Wiley, 1993.
- [2] D. W. Strangway, W. A. Gose, G. W. Pearce, and J. G. Cames, "Magnetism and the history of the moon," in *Proc. 18th Ann. Conf. Magn. Mater.*, 1973, pp. 1178-1197, Pt. 2.
- [3] D. Gubbins and E. Herrero-Bervera, *Encyclopedia of Geomagnetism and Paleomagnetism (Encyclopedia of Earth Sciences Series)*. New York: Springer-Verlag, 2007.
- [4] G. Kletetschka, P. J. Wasilewski, and P. T. Taylor, "Mineralogy of the sources for magnetic anomalies on mars," *Meteor. Plan. Sci.*, vol. 35, pp. 895-899, 2000.
- [5] P. Kearey and M. Brooks, *An Introduction to Geophysical Exploration*. Oxford, U.K.: Blackwell, 1991.
- [6] J. M. D. Coey, S. Mørup, M. B. Madsen, and J. M. Knudsen, *J. Geophys. Res.*, vol. 95, p. 14423, 1990.
- [7] P. P. K. Smith, "Spinodal decomposition in a titanomagnetite," *Am. Mineral.*, vol. 65, pp. 1038-1043, 1980.
- [8] D. H. Lindsley, "Some experiments pertaining to the magnetite-ulvospinel miscibility gap," *Am. Mineral.*, vol. 66, pp. 759-762, 1981.
- [9] I. Lucas, M. D. Michelena, R. P. del Real, V. de Manuel, J. A. Plaza, M. Duch, J. Esteve, and H. Guerrero, "A new single-sensor magnetic field gradiometer," *Sens. Lett.*, vol. 7, no. 8, pp. 563-570, 2009.
- [10] R. Sanz, M. Cerdán, A. Wise, M. E. McHenry, and M. Díaz-Michelena, *IEEE Trans. Magn.*, to be published.
- [11] B. A. Wechsler, D. H. Lindsley, and C. T. Prewitt, "Crystal structure and cation distribution in titanomagnetites ( $\text{Fe}_{3-x}\text{Ti}_x\text{O}_4$ )," *Am. Mineral.*, vol. 69, pp. 754-770, 1984.
- [12] U. Bleil, *An Experimental Study of the Titanomagnetite Solid Solution Series Pageoph.* Basel: Birkh user Verlag, 1976, vol. 114.
- [13] K. M. Creer, J. Ibbetson, and W. Drew, *Geophys. J. R. Astr. Soc.*, vol. 19, pp. 93-101, 1970.
- [14] R. Aragon, R. H. McCallister, and H. R. Harrison, *Contrib. Mineral. Petrol.*, vol. 85, pp. 174-185, 1984.
- [15] H. Flood H and D. G. Hill, *Z Elektrochem* vol. 61, pp. 18-24, 1957.
- [16] G. D. Price, *Am. Mineral.* vol. 66, pp. 751-758, 1981.
- [17] A. Hsiao, M. E. McHenry, D. E. Laughlin, M. J. Kramer, C. Ashe, and T. Okubo, "The thermal, magnetic and structural characterization of the crystallization kinetics of amorphous soft magnetic materials," *IEEE Trans. Magn.*, vol. 38, pp. 2946-2948, 2002.